Short-Term Carbon Intensity Forecasting

Master's Thesis

for acquiring the degree of
Master of Science (M.Sc.)
in Information Systems

Humboldt-Universität zu Berlin
School of Business and Economics
Chair of Information Systems

Carl Tramburg
(545465)
Berlin, May 13, 2024

1st Examiner:	Dr. Alona Zharova
2nd Examiner:	Prof. Dr. Stefan Lessmann

Abstract

Short-term carbon intensity forecasting is crucial for optimizing energy consumption towards carbon emissions. This thesis focuses on predicting carbon intensity across the four German Transmission System Operators (TSO) zones: 50Hertz, Amprion, Tennet, and TransnetBW. The data sets are enriched by weather and market price data. The accuracies of ARIMA, SARIMA, and Temporal Fusion Transformer (TFT) models is assessed in all four regions. Results indicate that the univariate SARIMA model consistently outperforms both ARIMA and TFT models across all TSO zones, utilizing an input window of 28 days and a forecast length of 24 hours.

Additionally, this study presents a smart home solution designed to provide users with real-time carbon intensity forecasts. The visualization in Home Assistant and the backend are developed in an open-source microservice architecture approach, allowing for flexible adjustments and integration of various forecasting methods.

Contents

List of Abbreviations

ADF	Augmented Dickey-Fuller
ANN	Artificial Neural Network
(S)ARIMA	(Seasonal) AutoRegressive Integrated Moving Average
API	Application Programming Interface
CEF	Carbon Emission Factors
CI	Carbon Intensity
EU	European Union
EEX	European Energy Exchange
ENTSO-E	European Network of Transmission System Operators for Electricity
DWD	Deutscher Wetterdienst (German Meteorological Service)
GHG	Greenhouse gases
GWP	Global Warming Potential
GUI	Graphical User Interface
IPCC	Intergovernmental Panel on Climate Change
LASSO	Least Absolute Shrinkage and Selection Operator
LSTM	Long Short-Term Memory
MAPE	Mean Absolute Percentage Error
MLP	Multi-Layer Perceptron
PSO-ERT	Particle Swarm Optimised - Extremely Randomised Trees
RMSE	Root Mean Squared Error
RNMSE	Root Normalized Mean Squared Error
TFT	Temporal Fusion Transformer
TSO	Transmission System Operator

List of Figures

List of Tables

1 Introduction

The electric power industry accounted for 37% of Germany's greenhouse gas emissions in 2021, making it the largest contributor to the country's carbon footprint (German Environment Agency, 2023). In order to achieve the targets set out in the Paris Agreement, Germany must reduce its carbon emissions by 55% by 2030, compared to 1990, and realize net zero green house gas emissions by 2050. In its *Climate Action Plan 2050*, the German government has stated the transformation of the energy sector almost completely to renewable energy as one of its strategies. The plan also outlines "that electricity demand will in the long term be significantly higher than today [...] as a result of the increasing electrification of the transport sector and the heat supply to buildings" (Federal Ministry for the Environment and Safety, 2016). Both, increasing demand for electricity and replacement of fossil fuels with renewable energy sources, will place greater pressure on the electricity grid and its tranformation. With respect to a carbon-free future, renewable energy sources must replace fossil fuels as the primary source of electricity generation and must also cover increased demand from the transportation and heating sectors. However, the inherent variability from solar and wind power have a significant impact on the carbon emissions of the electricity generation. The fluctuating nature of these renewable energy sources makes it challening to consumers to plan their electricity usage in a way that minimizes their carbon footprint.

One solution to this problem is providing consumers with real-time information on the carbon intensity of the electricity grid. Thereby enabling them to make informed decisions about their electricity consumption, and therefore also about their carbon footprint. This information can be used to optimize a consumer's carbon footprint by shifting electricity usage to times when the generation is greenest. Smart Homes are a promising technology to achieve this goal and they help reducing the carbon footprint of households (Louis et al., 2014). For example, a smart home could be programmed to run energy-intensive appliances, such as washing machines and dishwashers, or charge a electric vehicle when the carbon intensity of the grid is low. This would not only reduce the households's carbon footprint but also helps balancing the grid by shifting electricity usage to times when renewable energy sources are abundant (Gleue et al., 2021).

This thesis provides greater granularity to the German electricity grid by forecasting the carbon intensity of each of the four German Transmission System Operator (TSO) zones based on electricity generation data, weather data and electricity market prices. Additionally, this thesis explores the use of transformers in carbon intensity forecasting. Furthermore, this thesis contributes by presenting a smart home implementation that forecasts carbon intensity for the next 24 hours, tailored to the user's geographic location within the German electricity grid.

The remaining sections of the thesis are structured as follows. The Literature Review delves into existing research on carbon intensity forecasting, analyzing current models and methodologies while providing a comparison of state-of-the-art studies. The Methodology chapter details the models used for forecasting carbon intensity and explains the evaluation process The Data section describes data retrieval and preparation from the ENTSO-E and DWD APIs, followed by data analysis. The Results chapter presents the outcomes and performance of the models. In the Implementation into Home Assistant chapter, the system architecture and integration of the forecasting model into a real-world application are described. The Discussion section compares the results with previous research and assesses the implications. Finally, the Conclusions summarizes the study and outlines future research directions..

2 Literature Review

The domain of energy market research has been gaining attention as the volaility from renewables and the transition to a more sustainable energy system is increasing. The literature on carbon intensity forecasting is vast and varied, with a range of methodologies and applications. This section provides an overview of the state of the art in carbon intensity forecasting, focusing on the methodologies and applications of the most recent studies.

Leerbeck et al. (2020a) present a methodology for short-term CO2 emissions forecasting in power grids using machine learning. Focusing on the Danish bidding zone DK2, it incorporates a dataset of 473 variables, reduced to under 30 using LASSO and feature selection algorithms. Three linear regression models are combined into a final model with Softmax weighted average and ARIMA for residual correction. Results demonstrate forecast errors varying between 0.095 and 0.183 for average emissions and 0.029 – 0.160 for marginal emissions, depending on the forecast horizon. Bokde et al. (2021) present two time-series decomposition methods: a statistical approach that identifies seasonal and trend components, and an ensemble empirical mode decomposition (EEMD) that produces intrinsic mode functions. In a 48-hour forecasting window, the authors compare the performance of various forecasting models in combination with these decomposition techniques. By testing across multiple country grids, a combination of a feedforward neural network and a statistical approach outperformed the other models, achieving a MAPE of 11.47%.

The project "CarbonFirst - Decarbonizing Cloud Computing" (Laboratory for Advanced Systems Software, 2021) presents two papers in the field of CI forecasting: Maji et al. (2022b) present an open-source system architecture approach DACF - *Day-Ahead Carbon Forecasting*. The model employs ANNs, fed with historical energy generation data and weather forecacast data, to calculate the carbon intensity for the next 24 hours. DACF considers short-term (hourly) and long-term (seasonal) patterns to predict energy generation per production type indivdually. Subsequently, each forecasted generation type is multiplied by its respective carbon emission factor to compute the carbon intensity of the designated region. DACF attains an average Mean Absolute Percentage Error of 6.4% across all six evaluated regions, with Germany specifically reg-

istering a MAPE of 9.08%. Building upon their foundational work, Maji et al. (2022a) employed a two-tier hierarchical methodology to forecast the carbon intensity for up tp 96 hours. In the first tier, similar to the DACF framework, ANNs are utilized to individually forecast the output of various types of energy generation. Subsequently, in the second tier, a Convolutional Neural Network-Long Short-Term Memory (CNN-LSTM) combines the initital forecasts with historical carbon intensity data and meteorological forecasts to estimate the carbon intensity for a period extending to 96 hours. The authors state that this strategy extends model robustness against noise in the input data and improves resiliency against missing data. *CarbonCast's*, MAPEs range between 4.80 and 13.93% in six evaluated regions, but is not outperforming DACF in terms of one-day forecast accuracy.

Incorporating the dynamics of electricity flows between regional power grids, the *Carbon Intensity Forecasting for Cross-border Grids (CFCG)* model is introduced. This model is composed of two machine learning submodels: a Graph Neural Network (GNN) designed to capture the spatial dependencies from one-hop neighbor grids and their impact on carbon intensity, and a LSTM model aimed at uncovering the temporal patterns in data fed with multiple periodic time granularities. The CFCG method demonstrates an improvement of 26.07% in average MAPE for 28 counties compared to DACF, underscoring its effectiveness in a complex, multi-national energy systems. However, DACF proves higher performance in less-integrated grids.

Riekstin et al. (2018) employed LSTM networks to forecast day-ahead greenhouse emissions, targeting smart home energy management systems. In two scenarios, with a dishwasher and a electric vehicle, the authors show, that a reduction in GHG was able without significant impact on the user's behavior. The performance of the employed LSTM reached a MAPE of 2% when the region's electricity mix is mostly based on fossil fuels, and 12% in regions with a high share of renewable energies.

Lowry (2018) utilized both daily and weekly AR models, alongside a three-layered ANN with four lagged input capturing observations from four consecutive periods, immediately preceding, one day, two days, and one week before the forecast. The models were trained on the UK grid's carbon intensity data. The ANN model achieved a root mean squared error of 0.056, while the daily seasonal AR model had an RMSE

of 0.058 for a 24-hour forecast on a half-hourly dataset. The models did not rely on any exogenous data sources. In the German grid Huber et al. (2021) introduced a smart charging system to reduce CO2 emissions from electric vehicle charging. Initially, a linear regression model calculates the marginal emission factors. These factors are then fed into a feed-forward multilayer perceptron that forecasts the carbon intensity for the next 8 hours. The MLP achieved a MAPE of 3.83%.

Furthermore, Great Britain's national grid operator provides an API service for carbon intensity forecasting. The forecasting method of Bruce et al. (2021) employs an ensemble of supervised regression models predicting the carbon intensity of the national and regional grids for up to 3 days.

As a commercial application, *Electricity Maps* (Electricity Maps, 2024) provides CO2 forecasts to paying customers, though the forecasting approach remains undisclosed. In addition, Electricity Maps offers a real-time carbon intensity map and serves as a data source for the Home Assistant energy card, an open-source smart home solution (Team, 2020). Based on the user's location, Home Assistant can display the real-time CO2 intensity of the connected electricity grid.

Likewise, Watttime (2023) provides a commercial API with a horizon of up to 72 hours. The method is disclosed and the API is available for developers. Watttime also offers a forecasting service for paying customers. At Google (Radovanović et al., 2022) developed *CICS - Carbon-Intelligent Computing System*, which employs textquotecarbon-aware Virtual Capacity Curves in order to shift flexible workloads to low-emission periods with a windows of 24 hours and accross all their data centers and regions.

In Table 1 research is summarized, consisting information of the models used, the performance metrics achieved, as well as the forecasting horizon and targeted geographical zones of each study. Additionally, it indicates the availability of open-source code and the utilization of smart home data, transformers, TSO zones, and weather data, providing an overview of current research trends and methodologies.

	Reference	Model	Period	Performance Metric	Data Categories	Geozones	Open Source Code	Smart Home	Transformers	TSO zones	Weather Data
academic	Aryai and Goldsworthy (2023)	PSO-ERT	24h	RMSE (25.4 - 165.7)	generation, demand	NSW, QLD, SA, TAS, VIC	-	-	-	-	+
	Zhang and Wang (2023)	GNN + LSTM	24h	MAPE (12.92%)	generation, cross-boarder flows	28 european countries	+	-	-	-	-
	Maji et al. (2022b)	ANN	24h	MAPE (6.4%)	generation	CA, DE, TX, ISNE, PJM, SE	+	-	-	-	+
	Maji et al. (2022a)	ANN, CNN-LSTM 2	96h	MAPE (9.96%)	generation	CA, PJM, TX, NE, SE, DE	+	-	-	-	+
	Leerbeck et al. (2020a)	Lasso, FFS, ARIMA, ARIMAX	24h	NRMSE (0.095 - 0.183)	generation, demand, cross-border flow	DK2	-	-	-	-	+
	Leerbeck et al. (2020b)	state-space model	24h	CO2 reduction (16%)	marginal CO2 emission	DK2	-	-	-	-	+
	Bokde et al. (2021)	ARIMA, FFNN, SVM, PSF, DPSF	48h	MAPE (11.47%)	generation, demand cross-border flows	FR, DE, NO, DK, PO	-	-	-	-	-
	Riekstin et al. (2018)	LSTM, RNN	24h	MAPE (2%)	generation	PJM, Ontario, FR	-	+	-	-	-
	Lowry (2018)	AR, ANN	24h	RMSE (0.056)	generation	UK	-	-	-	-	-
	Huber et al. (2021)	MLP	8h	MAPE (3.83%)	generation, load	DE	-	-	-	-	+
commercial	Bruce et al. (2021)	supervised ML regression	48h	n/a	generation	UK	-	-	-	-	+
	Watttime (2023)	n/a	72h	n/a	generation, demand, price	US	-	-	-	-	+
	Electricity Maps (2024)	n/a	24h	n/a	generation, cross-border flows. price	Worldwide	-	-	-	-	+
	Our Contribution	ARIMA, TFT	24h	MAPE	generation, price	50Hertz, Amprion, Tennet, TransnetBW	+	+	+	+	+

Table 1: Literature Review Summary

NSW: News South Wales, QLD: Queensland, SA: South Australia, TAS: Tasmania, VIC: Victoria, CA: California, DE: Denmark, ERCO: ERCOT, ISNE: ISO New England, PJM: Pennsylvania, New Jersey, Maryland, TX: Texas, NE: New England, SE: Sweden, FR: France, NO: Norway, DK: Denmark, PO: Poland, UK: United Kingdom, US: United States, EU: European Union, GB: Great Britain

3 Methodology

This thesis examines two forecasting models that are applied to the four regional electricity transmission networks in Germany: a statistical ARIMA model and a deep learning-based Temporal Fusion Transformers model. The ARIMA model provides a baseline for comparison, whereas the TFT offers a complex, multi-input forecasting method. The forecasting approach is based on the research of Riekstin et al. (2018), where the authors state an optimal input window of 28 days for a 24 hour forecast. The preprocessed data, from the 4 section, is split into training and test sets, with the training set spanning from January 2015 to February 2022 and the test set from March 2022 to February 2024. The TFT models is trained on the training set. Both models are evaluated with a rolling window cross-validation approach, with an input window of 28 days and a test window at 24 hours. The evaluation metric is the Mean Absolute Percentage Error. The empirical results are discussed in Section 5.

3.1 ARIMA

Autoregressive Integrated Moving Average is a popular statistical approach for time series forecasting. ARIMA models are prominent for their mathematical simplicity and accuracy in short-term forecasting. However, they exhibit limitations in complex scenarios due to their inflexibility in responding to rapid changes, in contrast to deep learning models (Kontopoulou et al., 2023; Ospina et al., 2023) The model consists of three components: Autoregression (AR), Differencing (I), and Moving Average (MA). The Autoregression component refers to the use of previous values in the time series as predictors for the future values, where parameter p denotes the number of lag observations included in the model. Parameter d (Differencing component) involves differencing the time series a certain number of times to make it stationary, addressing trends in the data. The Moving Average uses the dependency between an observation and a residual error from a moving average model applied to lagged observations, where parameter p represents the size of the moving window. Equation 1 represents the general form of an ARIMA model.

$$y_t = c + \sum_{i=1}^{p} \phi y_{t-1} + \sum_{i=1}^{p} \theta_i y_{t-p} + \varepsilon_t \tag{1}$$

The model's assumption includes stationarity. Time series are stationary, if statistical properties such as mean, variance, and autocorrelation are constant over time. This assumption can be checked using the Augmented Dickey-Fuller (ADF) test. For all four data sets, the carbon intensity time series are stationary with ADF-statics less than -15 (p-value <0.05).

Another aspect of ARIMA forecasting is seasonality, a periodic pattern that repeats over a specific time interval. Extended by a seasonal contribution, SARIMA models can incorporate such patterns in the forecasting. The seasonal extension is denoted by $(P, D, Q)_m$ where P, D, Q are similar to the ARIMA parameters, and m represents the seasonal period. For example, a seasonal period of m=24 denotes a daily pattern in an hourly time series. Seasonality can be examined with the autocorrelation function (ACF) and partial autocorrelation function (PACF) plots.

As Figure 1 shows, the ACF plot for the Tennet zone exhibits a significant spike at lag 24, indicating a daily seasonality pattern. As well, the ACF plot show further spikes in patterns of 24 hour steps, indicating also 48 hours seasonality and weekly seasonality. These findings are also statet by Lowry (2018), where a daily and weekly AR model reached RMSEs of 0.058 and 0.066, respectively.

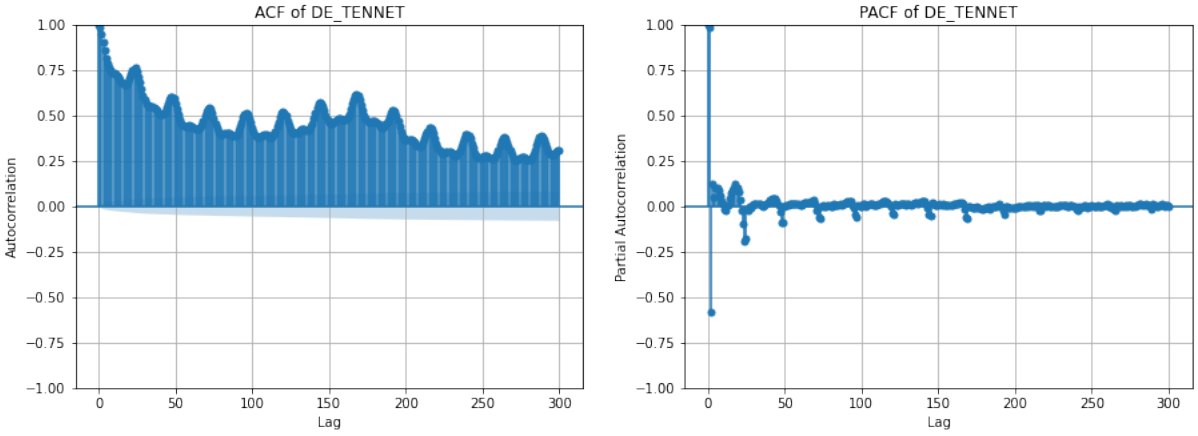

Figure 1: ACF and PACF in Tennet zone

The ARIMA parameter determination involves identifying the optimal parameters

(p, d, q) based on the Akaike Information Criterion (AIC) and diagnostic checks for autocorrelation in the residuals.

The AR, I and MA components are calculated through a stepwise approach, utilizing the *auto_arima* function from the Python library *pmdarima* (Smith et al., 17).

For every forcasting window consisting of 28 days input observations and 24 hours forecast, the the parameter determination will be derived from the auto_arima function. Then, the ARIMA model is fitted on the training set and finally a forecast is made and evaluated against the actual values in the test set. The procedure is repeated in a rolling window approach for the entire test set The ARIMA model is implemented using the Python library *statsmodels* (Seabold and Perktold, 2010). As well, the seasonal daily SARIMA model employed by Lowry (2018) is evaluated on the test set to compare the performance of the ARIMA model with and without seasonality. The parameter of the seasonal model are $(p=4,d=0,q=0)(P=4,D=0,Q=0)^{24}$.

3.2 Temporal Fusion Transformers

Attention-based Transformer mechanisms have gained popularity in natural language processing due to their ability to avoid recurrence and implement a self-attention mechanism that captures relationships between features with less training effort (Vaswani et al., 2017). Temporal Fusion Transformers (TFT) employ the self-attention mechanism of Transformers alongside recurrent layers (Lim et al., 2021). The architecture of TFT consists of following new components: gating mechanism, variable selection networks, static covariate encoders and temporal processing. A Gated Resdiual Network serves as gating and variable selection mechanism in order to exclude irrelevant input features and adjust the complexity of the non-linear transformation based on the data characteristics. The static covariate encoders integrates static data, like datetime features, in order to enrich the data with static information, improve variable selection and local processing. The temporal processing component is responsible for extracting long-termn dependencies by employing a self-attention mechanism and a sequence-to-sequence layer for learning about the short-term relations in the data. On multiple datasets Lim et al. (2021) showed that the TFT model outperforms other

deep learning models. Furthermore, TFT analyzes the importance of input features for the features that "intuitively play a significant role in predictions" and visualizes the temporal patterns by plotting the attention weights across the forecast horizon.

The implementation of the Temporal Fusion Transformer (TFT) model utilizes the PyTorch Forecasting library (Beitner, 2023b). Parameter selection and implementation are based on the documentation and the work described by Beitner (2023a). The model employs static features: for the data sets, the statics features are date time variables such as, day of the week, hour of the day and month of the year. These features are used in both the encoder and decoder of the model.. In other words, known future values are included in the prediction. Firstly, the Python library expects a *TimeSeriesDataSet* object. The data are categorized accordingly into static and dynamic as well as known and unknown features. Besides, TFT expects a group identifier, which is the TSO zone in this case. Afterwards, the *TemporalFusionTransformer* model is created and trained on the training set. Accross all data sets, the model's hyperparameters are aligned. The learning rate (0.03) determines how much the weights of the model are updated during the training to the estimated error. Two attention heads are used to incorporate on differents parts of the encoding sequence. As loss function, the MAPE is used, which will be described in the evaluation section.

The model is fitted on the training set and evaluated on the test set in the same procedure as the ARIMA model.

3.3 Evaluation

Initially, the datasets are divided into training and test sets. The Temporal Fusion Transformer model requires training, so it is fitted using the training data. In contrast, statistical models like ARIMA do not necessitate explicit training. Instead, ARIMA optimizes its parameters iteratively on the test data, adjusting at each forecasting step.

Afterwards, the evaluation is conducted on the test split using rolling-window cross-validation with fixed input and predication length (Hyndman and Athanasopoulos, 2021). In this method, the first 28 days ($28 \times 24 = 672$ observations) are used as the initial training window to predict the subsequent day (24 observations). After each prediction, the training window rolls forward by one day, maintaining the temporal

sequence. This process is repeated throughout the entire test period to validate both models performance over multiple consecutive days. The decision to use a 28-day training window stems from the research of (Riekstin et al., 2018) and their preliminary data set analysis and test on different window sizes. As well, as the goal of this thesis is to implement a short-term forecasting smart home solution, the retrieval of longer periods from the ENTO-E API requires substantial time.

For each TSO zone and model, the Mean Absolute Percentage Error is calculated to quantify the prediction errors. MAPE is selected because it provides a relative and scale-independent metric that allows for comparison in all data sets, as theses vary in the magnitude of the CI values. As well, MAPE shows to be the most common metric in the Literature Review, so the results can be compared to other studies.

The MAPE formula is described as:

$$\text{MAPE} = \frac{1}{n} \sum_{t=1}^{n} \left| \frac{y_t - \hat{y}_t}{y_t} \right| \times 100$$

where: n is the total number of observations, y_t represents the actual value at time t, and $\hat{y}_t$ denotes the predicted value at time t.

4 Data

This study's data is based on two primary sources: energy market data from the European Network of Transmission System Operators for Electricity (ENTSO-E) and weather data provided by the German meteorological service (DWD). The following sections describe the data collection, data preparation, and feature creation processes, as well as the subsequent data analysis. The data encompasses the period from January 2015 to February 2024.

4.1 Data Collection

4.1.1 Electricity Market Data

Generation Data

The basis for calculating the carbon intensity is the energy generation data, which will then be multiplied by the respective carbon intensity factor (CEF). The energy generation data is retrieved from ENTSO-E API (Pecinovsky and Boerman, 2021). The provided dataset are collected at 15-minute resolution for each type of generation in Megawatts. Depending on the TSO zone, the number of generation types varies: 14 in the 50Hertz grid, 15 in the Transnet area, and 16 in the grids of Tennet and Amprion. The API Service provides the raw data as multi-column Pandas DataFrame with *aggregated generation* and *aggregated consumption*. Consumption is omitted as the thesis' goal is to focus on the carbon intensity from electricity generation. Subsequently, the data resolution is converted from 15-minute intervals to hourly intervals. This transformation is accomplished by resampling the 15-minute data points and aggregating the generation totals, summing them up into hourly data points. Additionally, the unit changes from megawatts to megawatt-hours.

Day-Ahead Price

As well, day-ahead price data from region DE_LU are included in the datasets. Paraschiv et al. (2014) state, that renewables energy resources increase the exploratory significance for day-ahead prices. This implies that, due to lower marginal costs, renewables

have a significant negative impact on day-ahead prices and, vice versa, it is expected that day-ahead prices influence the emissions rate in the grid, and therefore improve the forecasting accuracy of the carbon intensity. In other words, low day-ahead prices are associated with low carbon intensity, as the share of renewables in the generation mix is higher. From the data, it is also obervable that the feature and the carbon intensity are positively correlated. The day-ahead prices are also provided from ENTSO-E API on an hourly resulotion. Price data for the german zone are split into two bidding zones that switched in October 2018 due to regulatory decree of the EU (Graefe, 2023). From January 2015 to September 2018 the dayahead price are retrieved for the bidding zone *Germany, Austria, Luxembourg (DE_AT_LU)*. Since October 2018 day-ahead price refers to bidding zone *DE_LU*.

4.1.2 Weather Data

Weather plays an essential role in the performance and predictability of renewable energy sources, primarily wind and solar power. The inherent volatility of these energy sources is largely due to their direct dependence on the weather conditions. For instance, solar energy production is significantly affected by cloud cover and solar radiation, while wind energy generation is influenced by wind speed. Accurate weather forecasting is therefore essential to predict the availability and variability of these renewable energies. State-of-the-art research has shown that weather data can improve the accuracy carbon intensity forecasts (Maji et al., 2022b; Leerbeck et al., 2020a). The weather data are retrieved with Python Package *wetterdienst* (Benjamin Gutzmann and Andreas Motl, 2023) that incorporated the *ClimateDataCenter* by the DWD, (Deutscher Wetterdienst, 2023). Each TSO zone in Germany is associated with one specific DWD weather station that is located inside the geographic area of the zone. These stations were selected based on their ability to provide comprehensive historical data for the corresponding data period. Due to the design of DWD data, these stations must also be able to provide obervation data for *recent* (last 500 to yesterday) and *now* (yesterday up to last hour) perdiods. As for a real time forecasting, the weather data must be preprocessed and merged in order to create an hourly dataset. More specific, for the period *now* the weather API does not provide an hourly resolution. Therefore,

Weather Feature	Description
radiation_global	sum of solar incoming radiation joule per square meter
sunshine_duration	Sunshine duration in seconds per hour
temperature_air_mean_200	2m air temperature in degrees Kelvin
temperature_dew_point_mean_200	Dew point temperature in degrees Kelvin
wind_direction	Mean wind direction in degrees
wind_speed	Mean wind speed in meter per second

Table 2: DWD weather features in periods historical, recent and now

the data must be aggregated to hourly resolution and then be merged with the historical hourly weather data from the *recent* period. The selected weather features are listed in Table 2.

4.2 Data Preparation

4.2.1 Missing Value Handling

To improve data quality and, consequently, the model's accuracy, missing values are analyzed and handled. In the power generation data from ENTSO-E no missing values are detected in none of the TSO zones. As well, the day-ahead price time series does not contain any missing values. Though, in contrary to the generation data, the price series starts at 5th January 2015, as the data supply on the ENTSOE-E platform was launched at 5th January 2015 (ENTSO-E, 2022). For this reason, the first 4 days of January 2015 are left out for the training of the model. The weather data, however, contain missing values. Sticking out most prominently the feature *sunshine duration* has a share of more than 25% over all 4 data sets. By examaning the hourly distribution of the missing values, it is noticeable that the missing values are mainly present during the night hours from 22 to 4. At these hours the values are replaced with zeros.

The remaining missing values are interpolated in two steps. First, the small gaps are interpolated with a cubic function for the maximum of 12 steps in both directions, back and forward (Silva, 2024; Lazzeri, 2021). In the second step, the remaining missing features are interpolated by the mean of the other 3 weather stations from that observation point. This approach is chosen on the basis that all stations are lo-

cated in the similar geographic area and the data shows strong and positive correlation for all features across the stations, except for wind features, that show weak positive correlation.

4.3 Carbon Emission Factors

The carbon intensity of a grid or a geographic zone is derived from the carbon emission factors associated with each energy source. CEF is a measure of the amount of carbon dioxide (CO2) emitted per unit of electric energy generated by a specific energy source. The carbon emission factor is expressed in grams of CO2-equivalents per kilowatt-hour (gCO2eq/kWh) of electricity generated, regarding different global warming potentials for various GHG. The carbon emission factor varies depending on the energy generation source. For example, renewable energies have none or low emissions, while fossil fuels have high carbon emission factors. In academia, different CEF schemes are incorporated: Maji et al. (2022b) use Scope 2 emissions, that only consider operational emissions, while Leerbeck et al. (2020a) use lifecycle emissions, that consider "the emissions associated with the production and use of a specific product, from cradle to grave, including emissions from raw materials, manufacture, transport, storage, sale, use and disposal." (World Resources Institute, 2023). This study employs lifecycle emissions based on data by the IPCC (Bruckner et al., 2014). The carbon emission factors are provided in Table 3.

The carbon intensity is calculated as the sum of the products of each energy source's emissions factor and its corresponding energy output divided by the total energy output. The calculation is described in equation 2:

$$CI = \frac{\sum(E_i * CEF_i)}{\sum E_i} \tag{2}$$

where E_i is the energy generation of the energy source i and CEF_i is the carbon emission factor of the energy source i.

Although the methodologies differ, they point in the same direction regarding the relative cleanliness of energy sources. All methodologies generally support the understanding that cleaner energy sources, such as wind, solar, and hydro, are less carbon-intensive compared to traditional fossil fuels like coal and natural gas. This conver-

Generation Type	Carbon Emission Factor
Biomass	230
Fossil Brown coal/Lignite	966
Fossil Coal-derived gas	1401
Fossil Gas	490
Fossil Hard coal	820
Fossil Oil	650
Geothermal	38
Hydro Pumped Storage	281
Hydro Run-of-river and poundage	24
Hydro Water Reservoir	24
Nuclear	12
Other	700
Other renewable	100
Solar	45
Waste	700
Wind Offshore	12
Wind Onshore	11

Table 3: Emission factor in gCO2eqkwh (median values)

gence is because, regardless of the scope or lifecycle stage considered, renewable energy sources produce fewer carbon emissions throughout their lifecycle.

4.4 Feature Engineering

Building an accurate and robust predictive model relies on the input features. In the context of forecasting carbon intensity, the creation and selection of appropriate features plays a vital role in capturing the underlying patterns and relationships within the data. As shown in Figure 2, the carbon intensity varies depending on the time of day and the season. The creation of datetime features that capture these patterns can help the model learn the relationships between the time and the target variable. The dataset is enriched with the following datetime features: hour, quarter, month, year, dayofweek, dayofyear, dayofmonth. Furthermore, the sinusoidal datetime features are added for hour and day. Sine and cosine transformation help to represent the periodic

pattern in time series. In an ordinal encoding, the hour represented by a number from 0 to 23 does not capture the cyclical nature, what is captured by this transformation (carpentries.org, 2023).

Apart from time-relevant features, energy market related features are added to the dataset. These domain-specific features can help the model learn the relationship between the energy market and the carbon intensity. Therefore, each dataset is enriched with the following features: share renewable energy, sum conventional energy, sum renewable energy, total emissions, sum generation.

4.5 Data Analysis

The four time series collected span from January 5, 2015, to February 29, 2024, with data recorded at hourly intervals, resulting in a total of 80,232 observations. Each German TSO zone features a variety of generation types. Throughout this period, the average carbon intensity varied across the zones:

The carbon intensity and its trend vary depending on the TSO zone. Generally, the share of renewable energies has increased in all zones. In the 50Hertz and Amprion TSO zones, the yearly average carbon intensity began in 2015 at levels higher than 600 gCO2eq/kWh and decreased to below 500 gCO2eq/kWh by 2023. Similarly, the carbon intensity for Tennet decreased during that period from 251 to 160 gCO2eq/kWh. In contrast, TransnetBW shows an increase in carbon intensity from 238 to 308 gCO2eq/kWh. This can be explained by an increase of the generation from fossil gas by 24th September 2020. Based on the two years before and after that day, the average generation from fossil gas increased by more than factor 10 leading to a 44% increase in the carbon intensity.

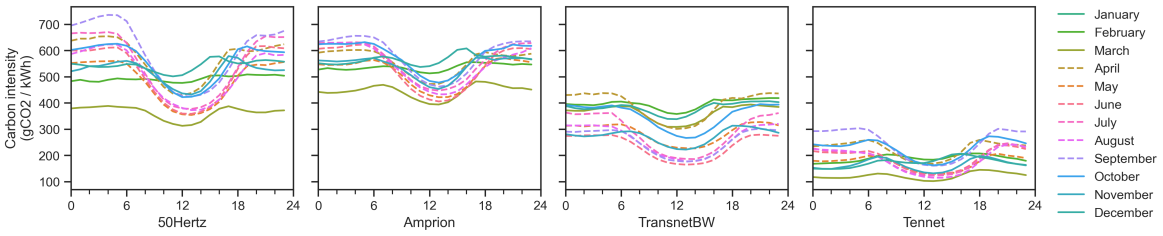

Figure 2: Daily average carbon intensity per TSO zone in 2022

4.5.1 Stationarity

Time series are stationary, if statistical properties such as mean, variance, and autocorrelation are constant over time, indicating that a time series is indepent of the time. Stationarity is a key assumption in time series forecasting models, such as ARIMA and SARIMA. Applying the Augmented Dickey-Fuller test, the null hypothesis of non-stationarity is rejected for almost all features, except the engineered features *year* and *sinus day of year* as these are dependend on time. As well, the features *Biomass*, *Other* and *Other Renewables* are non-stationary.

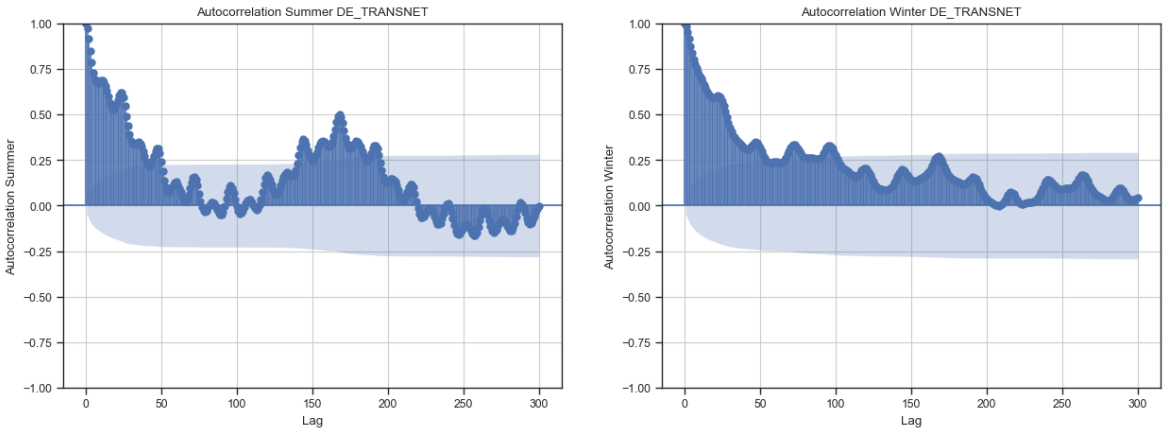

Figure 3: Autocorrelation function of carbon intensity in TransnetBW for summer and winter

4.5.2 Seasonality

Patterns that occur at regular intervals due to seasonal effects, holidays, or other cyclic factors are referred to as seasonality. These patterns result in regular and predictable fluctuations in the data over time. Understanding seasonality is important to understand the fluctuations in the data and improving forecasting accuracy. For instance, as shown in Figure 2, the carbon intensity varies depending on the time of day and the season. Over all four data sets, at night carbon intensity stays on a high level, while deacreasing to its lowest point at noon, and then, increasing back on high level over the afternoon. The amplitude is stronger in summer times than in winter. As well the autocorrelation function (ACF) and partial autocorrelation function (PACF) plots show the seasonality in the data. The ACF and PACF plot shows a strong correlation

at lag 24, indicating a daily seasonality. As well, it can be observed that a weaker correlation is present at lag 168, indicating a weekly seasonality. Another finding is, that the carbon intensity's autocorrelation varies among seasons. As an example, Figure 3 shows that the carbon intensity in TransnetBW in summer has a stronger autocorrelation than in winter. This can be explained by the higher share of solar generation in summer months and is observable in all TSO zones.

5 Results

The evaluation results of three forecasting models, ARIMA, SARIMA and Temporal Fusion Transformer, across the four TSO zones, are presented below. The predictive performance was measured using Mean Absolute Percentage Error, which is shown in Table 4. The models were evaluated on the test data set spanning from 1st march 2023 to February 29th 2024 with a rolling window forecasting approach. Each window comprised of 28 days (672 observations) input data and the subsequent 24 hours (1 day) forecast data.

TSO Zone	ARIMA	SARIMA $_{(4,0,0)(4,0,0,)24}$	TFT
50Hertz	24.85%	18.40%	28.97%
Amprion	19.65%	15.39%	22.79%
Tennet	36.55%	27.33%	37.42%
TransnetBW	26.04%	18.85%	23.03%

Table 4: Performance (MAPE) of ARIMA, SARIMA and TFT

The baseline model ARIMA shows it's best performance in the Amprion zone with a MAPE of 19.65% and the worst in the Tennet zone with a MAPE of 36.55%. The SARIMA outperforms the baseline and improves the forecasting accuracy in all TSO zones by 21% in Amprion to 27% in TransnetBW. The TFT model shows varying performances over all data sets, with the best accuracy in Amprion (22.79%) and TransnetBW (23.03%) area, even better than the baseline model. For the grids of 50Hertz and Tennet, the TFT model shows the worst performance a MAPEs of 28.97% and 37.42% As in this thesis' setup, with a rolling window approach and the training parameter setup equally for all datasets, the Transformers model is over all outperformed by the seasonal univariate model. Even though the training of all TFT models takes the longest time, this model shows the least accuracy.

Furthermore, from the test results, there are seasonal effects observable. For ARIMA, Table 5 shows that in winter the forecasting accuracy is better than in summer. Depending on the TSO zone, the effect ranges in an improvement of 42.53% in Tennet to 28.02% in Amprion. The SARIMA model, on the other hand, shows less differences. For this thesis setup, TFT shows no clear seasonal effect.

TSO Zone	ARIMA		SARIMA $_{(4,0,0)(4,0,0,)24}$		TFT	
	Summer	Winter	Summer	Winter	Summer	Winter
50Hertz	30.38%	17.74% (-41.61%)	17.73%	18.25% (2.94%)	29.47%	34.32% (16.47%)
Amprion	21.26%	15.30% (-28.02%)	14.89%	15.89% (6.75%)	23.95%	24.93% (4.09%)
Tennet	42.48%	25.35% (-40.33%)	25.19%	25.60% (1.62%)	33.65%	43.24% (28.51%)
TransnetBW	30.65%	17.62% (-42.53%)	19.46%	16.99% (-12.69%)	24.29%	20.25% (-16.65%)

Table 5: MAPE comparison per TSO zone in summer and winter (change in %)

As mentioned in the Methodology, the TFT serves interpretations of its predictions, such as variable importance and attention plot. The plot may help to better understand what features and which historical observations points have the highest impact on the prediction. ARIMA and SARIMA do not offer such interpretations.

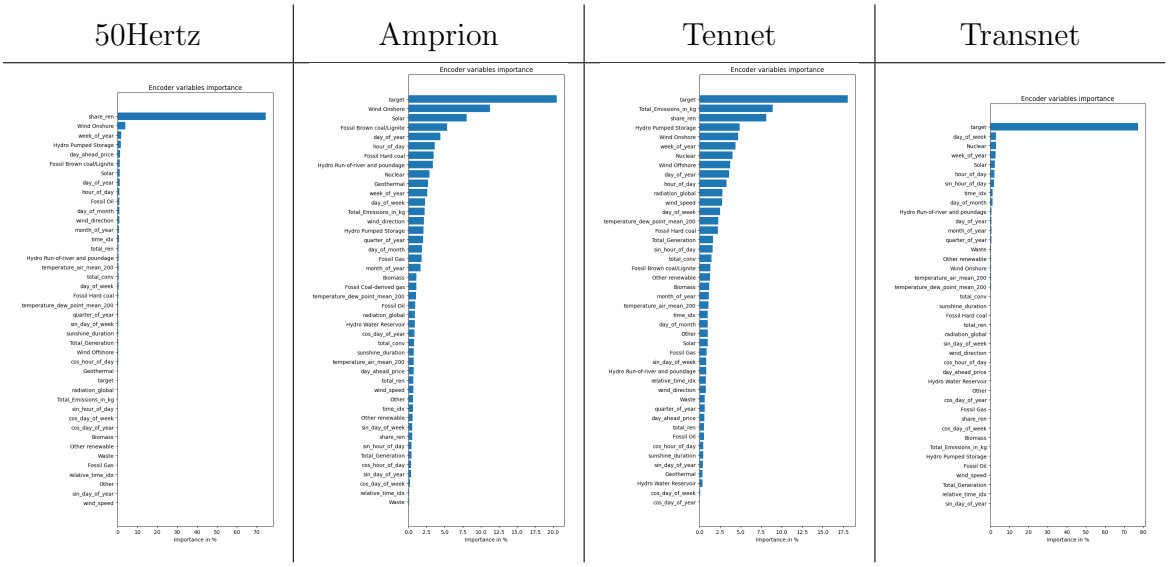

Figure 4: TFT encoder variable importance

From the "Encoder variable importance", it can be seen, that 50Hertz (share of renewables) and TransnetBW (target) show similar importance to almost only one variable. On the other hand, Amprion and Tennet show a distributed variable importance, with the target variable *carbon_intensity* being the most important. Figure 5 shows the importance of the historical observations for the prediction. The TSO zones do not have a common pattern. It can be observed, that, for example, over the 672 observation Transnet has high amplitude attentions in some observations. The other TSO zones show a more distributed attention over the 28 days.

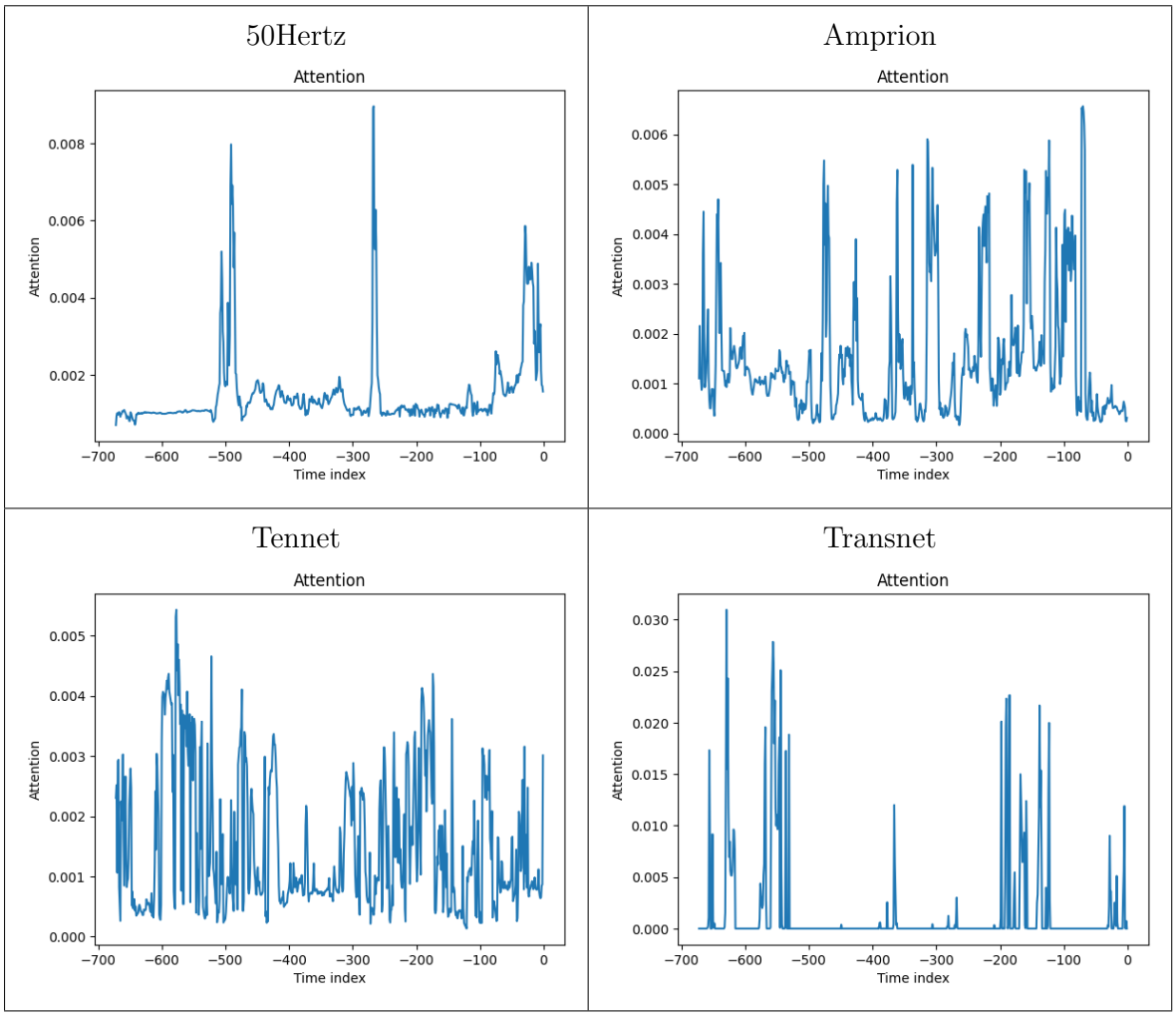

Figure 5: TFT attention plot

The most important engineered feature is *day_of_year*, followed by *hour_of_day*. From the perspective of data collection, weather features and day-ahead prices are less important to the model's variable interpretation.

From a date-time feature view, the most important engineered feature is *day_of_year*, followed by *hour_of_day*. From Figure 6 it can also be seen, that *week_of_day* and *cos_hour_of_day* are valuable engineered features for predicting the carbon intensity in the grid.

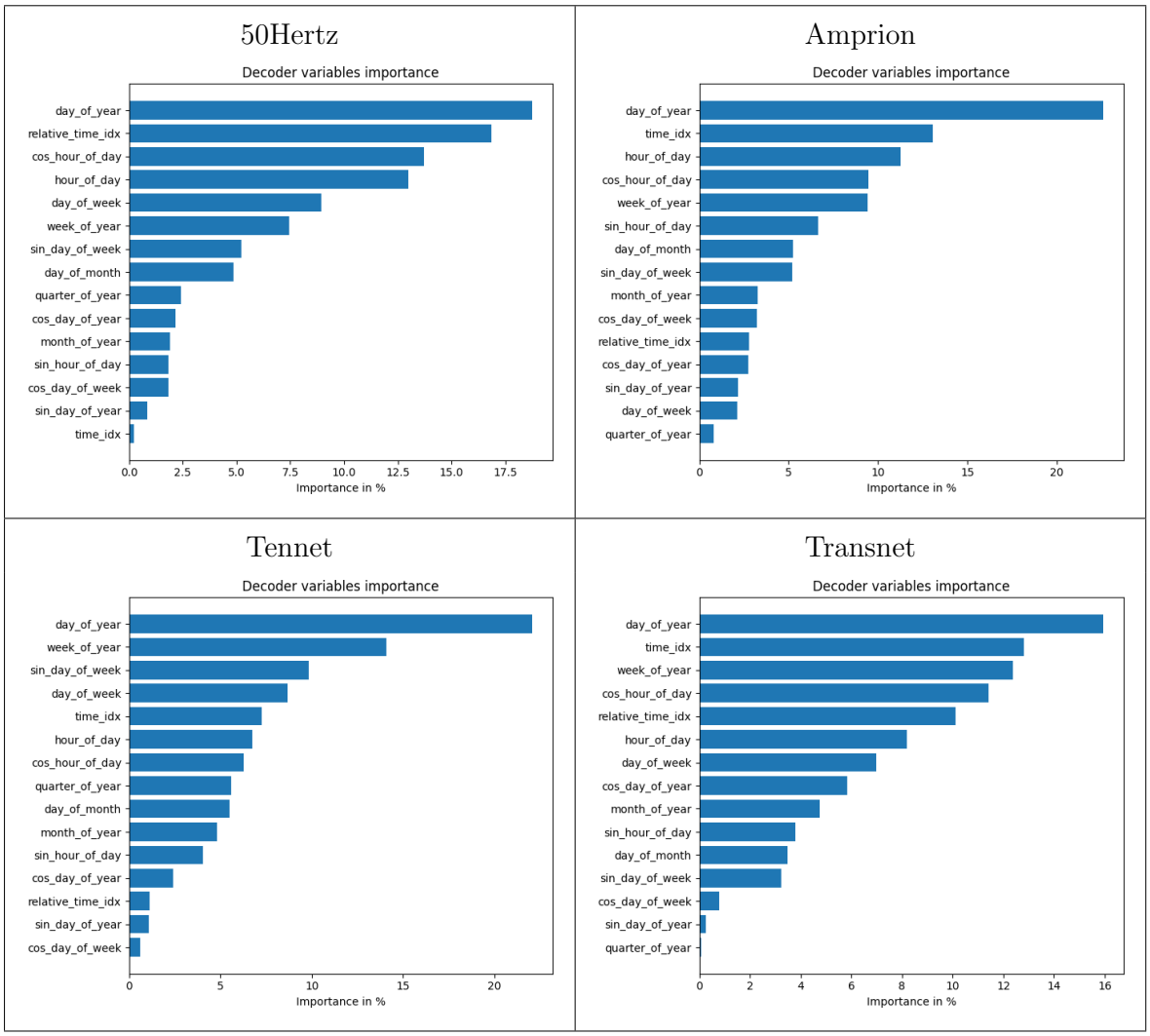

Figure 6: TFT decoder variable importance

6 Implementation into Home Assistant

One of this thesis' contributions is to design and present a real-world application in a smart home environment. *Home Assistant*, an open-source home automation software that offers a variety of individual customization options, is used as solution (Schoutsen, 2016).

6.0.1 System Design

The experimental system design is implemented using Docker (Merkel, 2014). The frontend is realized with a Home Assistant container, and the backend utilizes two containers: FastAPI as communication layer and a Python container as forecasting instance. The backend is designed as microservice architecture. The system architecture

is depicted in Figure 7.

Home Assistant visualizes and retrieves the forecasted carbon intensity data. This design visualizes the data with *Apex Charts* (Wiedemann, 2021) which can be installed from the community store *HACS* (Sørensen, 2020). To retrieve the forecast data from the backend, a RESTful Sensor is configured in Home Assistant. This sensor sends the system's geographic location from the system configurations as GET request.

The request is received by an API endpoint implemented with FastAPI. The endpoints are designed as a microservices. Firstly, another endpoint inside the FastAPI container is called to map the geolocation with the corresponding TSO zone. The mapping service initially loads the TSO zone data as *geojson* data from a Github repository [1].

After the location is mapped, the retrieving endpoint can call the actual forecast data from a shared file storage, where the third component saves hourly an updated forecast version for each transmission zone.

The forecasting container calculates the carbon intensity for each zone. It requests the energy market data and weather data from the corresponding APIs. The dataset is then preprocessed, enriched with the carbon intensity, and other features as described in Chapter 4. In this case, an ARIMA model is fit on the CI time series of 28 days to forecast the next 24 data points.

As the implementation is designed to be open-source and based on a microservice architecture, the system can be easily extended with additional forecasting models or features.

The system architecture is visualized in Figure 7. A graphical representation is shown in Figure 8.

[1] `https://github.com/tightdelay/Germany_EnergyGrid_DataSources`

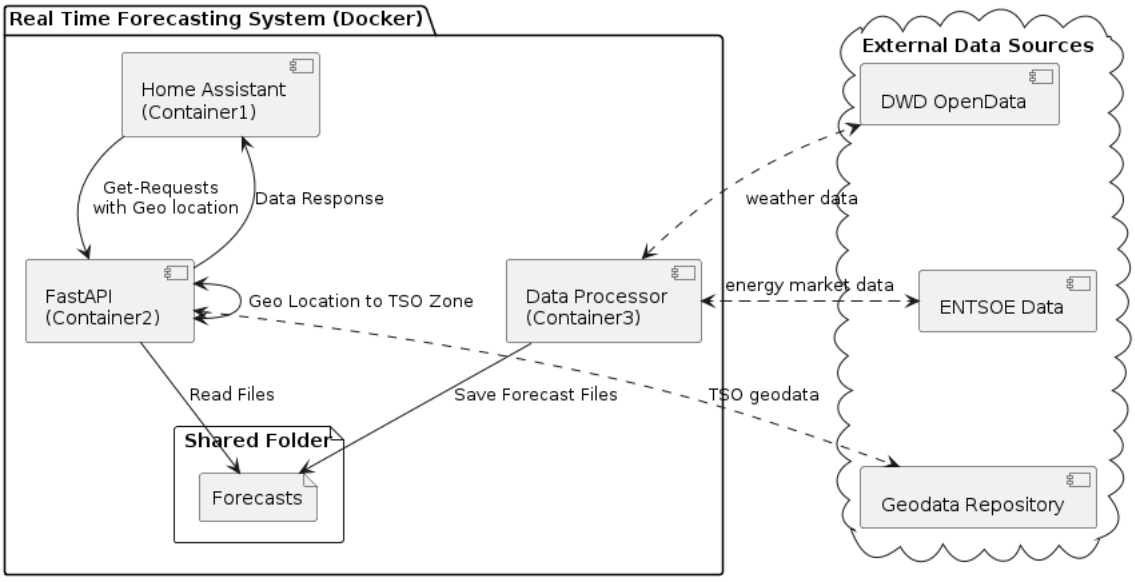

Figure 7: System Architecture

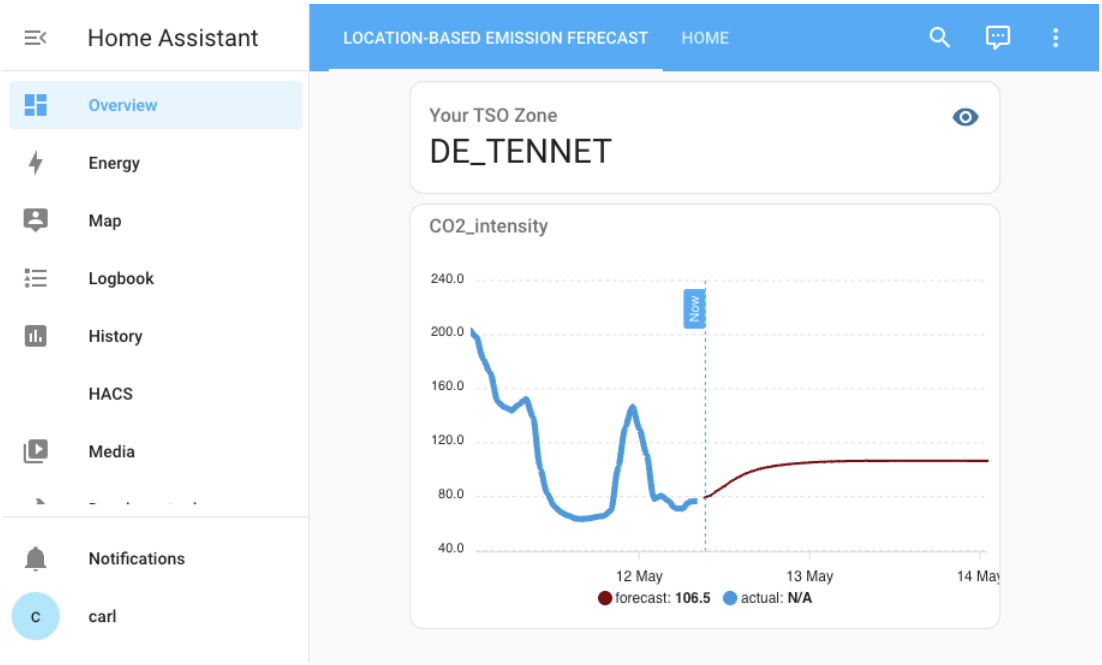

Figure 8: Graphical representation for Tennet in Home Assistant

7 Discussion

7.1 Interpretation

From the Results, it can be seen that the seasonal ARIMA model with the parameter $(4,0,0)(4,0,0)_{24}$ shows better performance than the ARIMA model in all TSO zones. The seasonal ARIMA model is able to capture the seasonality in the data and thus provides better results. ARIMA is not able to capture the seasonality in the data and thus provides worse results. When comparing all three models, in this study, univariate models perform better than the multivariate deep-learning TFT.

Also the results show that historical weather features and day-ahead prices do not significantly improve the performance of the TFT model. This might be due to the fact that the carbon intensity can be explained from the generation data and from time features, as seen Figure 6.

Still, the result is counterintuitive, as the Temporal Fusion Transformer model is expected to outperform the other models. Still, the result is supported by Kafritsas (2022): "Note: If your grouping static variable is not important, it is very likely your dataset can also be modeled equally well by a single distribution model (like ARIMA)." This is the case in this study, as a static variable is introduced to satisfy the model's requirements.

7.2 Comparison to other research

Like Riekstin et al. (2018) a 24 hour CO2 forecast based on data of the previous 28 days is calculated. In comparison, the best model, a seasonal ARIMA with the parameter (4,0,0)(4,0,0)24, is not as accurate as the LSTM in their study. Nevertheless it can be confirmed that the forecasting performance decreases when the the share of renewable energy increases.

In this study, the univarate model from Lowry (2018) has the highest accuracy, even though the calculation grounds only on the target feature itself. The author also implemented an ANN with multiple lag features that achieves small improvement in performance. This might imply that, due to its patterns, the carbon intensity time series can be predicted quite as good with univariate models.

7.3 Contributions

In this study, carbon intensity forecasting is applied to the four german transmission grids, and therefore bringing higher geographical granularity into the field. It is shown, that the regional grids vary in their levels of CI and in their sources of electricity generation. For each TSO zone a data set was created and enriched by weather data of a DWD station from that zone.

The study also contributes to the field of carbon intensity forecasting by applying a Temporal Fusion Transformer model to the data sets. The TFT was trained with data from January 2015 to February 2023 and tested on the last year of the collected data. The performance of the model was compared to an ARIMA and a Seaonal ARIMA model less accurate. This study points out that the best model is a seasonal ARIMA with the parameter $(4,0,0)(4,0,0)_{24}$ capturing the seasonality in the data and thus provides better results. The ARIMA model is not able to capture the seasonality.

Furthermore, this study contributes with a smart home system design, to inform a user about the upcoming carbon intensity. Based on the location in Germany, the approach offers a mapping between the grid and the user's locations and provides the CI values for the next 24 hours, employing an ARIMA forecast. The system is designed as open-source microservice architecture and can be adjusted for other methods.

7.4 Limitations

This study employed electricity generation data, market price data and weather data in order to forecast the carbon intensity in the four German transmission grids unsing a TemporalFusionTransformer model, an ARIMA and a SARIMA model.

The study has several limitations. Firstly, the data sources are expandable. For example, cross-border flow and weather forecast data are not included. These data were already mentioned in other studies for improving accuracy (Zhang and Wang, 2023; Maji et al., 2022a). Secondly, the TFT model can be improved by introducing further data sets, especially with static variables (Kafritsas, 2022). Such data can also come from the ENTSO-E API, that also provides forecasted features. Furthermore, per TSO zone, different model parameter could be tuned and evaluated.

The third limitation senses the comparison with other research. This thesis intro-

duced new regions and a new model to the field of carbon intensity forecasting. The comparison to other research is limited, as the data sets and the models differ. The application of LSTM (Riekstin et al., 2018), GNN (Zhang and Wang, 2023) and ANN (Maji et al., 2022b) models to the data sets could bring further insights into the performance of the models. The other way around, the generalization of SARIMA to other regions could be interesting, as well as the investigation of different input lengths for the forecasting.

The fourth limitation assigns the lack of databases usage in the smart home system design. This pitfall can bring latency to the system as databases are optimal as storage for structured data.

7.5 Future Research

Future research should dive deeper into different aspects of carbon intensity forecasting. To begin with, the calculation of the carbon intensity should be more standardized. In the literature, there are various approaches and sources that CI values are derived from. Especially for renewable energies, where the CI can zero or a positive number depending if operational or life cycle emission are considered. A standard can make methods more comparable. As well, a deeper analysis of the emissions can bring more accurate values. For example, the emissions from power plants of the same generation type vary, as the technology level differ, and therefore, the carbon emission factors. The ENTSO-E API provides plant-based data, which can be used for more precise values (ENTSOE, 2022).

Aside from the data sources, it can be interesting to investigate the effects of policy changes on the carbon intensity. For example, the nuclear and coal phase-out in Germany could have an impact in terms of emissions. Temporal Fusion Transformers can be prolific as it can incorporate future known event into the model Lim et al. (2021). Besides, when examinaning the phase-out, cross-border flows should be considered, as the emissions from other countries involved. Zhang and Wang (2023) already show that model improvement on the basis of one-hop neighbors can be achieved, but further hops should also be included, as the electricity grid is a interconnected system.

Furthermore, smart home systems can be researched to acquire the CO2 emission

savings. On the one hand, the system can take over the appliance control and shift the usage to times with lower carbon intensity. On the other hand, such system may help the transmission system operator to balance the grid by offering battery capacity from electric vehicles or storage. Gleue et al. (2021) already show that the consumers are willing to shift their usage based on flexible tariffs.

8 Conclusions

This thesis evaluates the forecasting performance of ARIMA, Seasonal ARIMA, and Temporal Fusion Transformers in predicting short-term carbon intensity levels across the four electricity grids in Germany and providing higher geographical granularity in the field of carbon intensity forecasting. The study integrates power generation data, day-ahead prices and weather observations revealing that the univariate Seasonal ARIMA model outperforms both the standard ARIMA and the Temporal Fusion Transformers.

An important contribution of this thesis is the development of a smart home application that utilizes data of the last 28 days to inform users about optimal carbon intensity for the next 24 hours. This tool has the potential to aid households in reducing their carbon footprint by aligning energy usage with periods of lower carbon intensity.

Despite its contributions, the study faces limitations, such as the limited exploration of cross-border electricity flows which could further refine the forecasting models. Future research could expand on these areas by integrating more dynamic data sources and exploring the impact of policy changes on carbon intensity. Additionally, extending the application to incorporate real-time decision-making in smart home systems could provide more practical utility and enhance user engagement.

References

Aryai, V. and Goldsworthy, M. (2023). Day ahead carbon emission forecasting of the regional national electricity market using machine learning methods. Engineering Applications of Artificial Intelligence, 123:106314.

Beitner, J. (2023a). Demand forecasting with the temporal fusion transformer. `https://pytorch-forecasting.readthedocs.io/en/stable/tutorials/stallion.html` [Accessed: 2024-02-19].

Beitner, J. (2023b). pytorch-forecasting.

Benjamin Gutzmann and Andreas Motl (2023). wetterdienst.

Bokde, N. D., Tranberg, B., and Andresen, G. B. (2021). Short-term co2 emissions forecasting based on decomposition approaches and its impact on electricity market scheduling. Applied Energy, 281:116061.

Bruce, A. R. W., Ruff, L., Kelloway, J., MacMillan, F., and Rogers, A. (2021). Carbon intensity forecast methodology. Technical report, National Grid Electricity System Operator (ESO) in partnership with Environmental Defense Fund Europe and WWF, Wokingham, UK; Department of Computer Science, University of Oxford. national: https://github.com/carbon-intensity/methodology/raw/master/Carbon

Bruckner, T., Fulton, L., Hertwich, E., McKinnon, A., Perczyk, D., Roy, J., Schaeffer, R., Schlömer, S., Sims, R., Smith, P., and Wiser, R. (2014). Technology-specific Cost and Performance Parameters [Annex III], pages 1329 – 1356. Cambridge University Press, Cambridge.

carpentries.org (2023). Feature engineering. `https://carpentries-incubator.github.io/python-classifying-power-consumption/02-feature-engineering` [Accessed 04-04-2024].

Deutscher Wetterdienst (2023). Climate data center. `https://cdc.dwd.de/portal/` [Accessed: 2023-02-13].

Electricity Maps (2024). Electricitymaps. https://www.electricitymaps.com/ [Accessed: 2024-03-15].

ENTSO-E (2022). Electricity market transparency. https://www.entsoe.eu/data/transparency-platform/ [Accessed: 2024-03-18].

ENTSOE (2022). Actual generation per generation unit [16.1.a]. https://transparency.entsoe.eu/content/static_content/Static%20content/knowledge%20base/data-views/generation/Data-view%20Actual%20Generation%20per%20Generation%20Unit.html [Accessed: 2024-05-10].

Federal Ministry for the Environment, Nature Conservation, B. and Safety, N. (2016). Climate action plan 2050—principles and goals of the german government's climate policy.

German Environment Agency (2023). Treibhausgasminderungsziele deutschlands. https://www.umweltbundesamt.de/daten/energie/energiebedingte-emissionen#entwicklung-der-energiebedingten-treibhausgas-emissionen [Accessed: 2023-12-23].

Gleue, M., Unterberg, J., Löschel, A., and Grünewald, P. (2021). Does demand-side flexibility reduce emissions? exploring the social acceptability of demand management in germany and great britain. Energy Research and Social Science, 82:102290.

Graefe, T. (2023). The effect of the austrian-german bidding zone split on unplanned cross-border flows. arXiv preprint arXiv:2303.14182.

Huber, J., Lohmann, K., Schmidt, M., and Weinhardt, C. (2021). Carbon efficient smart charging using forecasts of marginal emission factors. Journal of Cleaner Production, 284:124766 Elsevier.

Hyndman, R. J. and Athanasopoulos, G. (2021). Forecasting: principles and practice, 3rd edition. OTexts: Melbourne, Australia.

Kafritsas, N. (2022). Temporal fusion transformer: Time series forecasting with deep learning — complete tutorial. https://towardsdatascience.com/

temporal-fusion-transformer-time-series-forecasting-with-deep-learning-complete-tut
[Accessed: 2023-05-01].

Kontopoulou, V. I., Panagopoulos, A. D., Kakkos, I., and Matsopoulos, G. K. (2023). A review of arima vs. machine learning approaches for time series forecasting in data driven networks. Future Internet, 15(8):255.

Laboratory for Advanced Systems Software, U. o. M. A. (2021). Carbonfirst - decarbonizing cloud computing. http://carbonfirst.org/ [Accessed: 2023-12-12].

Lazzeri, F. (2021). Machine learning for time series forecasting with Python. Wiley,, Indianapolis, Indiana.

Leerbeck, K., Bacher, P., Junker, R. G., Goranović, G., Corradi, O., Ebrahimy, R., Tveit, A., and Madsen, H. (2020a). Short-term forecasting of co2 emission intensity in power grids by machine learning. Applied Energy, 277:115527.

Leerbeck, K., Bacher, P., Junker, R. G., Tveit, A., Corradi, O., Madsen, H., and Ebrahimy, R. (2020b). Control of heat pumps with co2 emission intensity forecasts. Energies, 13(11):2851.

Lim, B., Arık, S. Ö., Loeff, N., and Pfister, T. (2021). Temporal fusion transformers for interpretable multi-horizon time series forecasting. International Journal of Forecasting, 37(4):1748–1764.

Louis, J.-N., Caló, A., and Pongrácz, E. (2014). Smart houses for energy efficiency and carbon dioxide emission reduction. EnErgy, pages 44–50.

Lowry, G. (2018). Day-ahead forecasting of grid carbon intensity in support of heating, ventilation and air-conditioning plant demand response decision-making to reduce carbon emissions. Building Services Engineering Research and Technology, 39(6):749–760 SAGE Publications Sage UK: London, England.

Maji, D., Shenoy, P., and Sitaraman, R. K. (2022a). Carboncast: multi-day forecasting of grid carbon intensity. In Proceedings of the 9th ACM International Conference on Systems for Energy-Efficient Buildings, Cities, and Transportation, pages 198–207.

Maji, D., Sitaraman, R. K., and Shenoy, P. (2022b). Dacf: Day-ahead carbon intensity forecasting of power grids using machine learning. In Proceedings of the Thirteenth ACM International Conference on Future Energy Systems.

Ospina, R., Gondim, J. A., Leiva, V., and Castro, C. (2023). An overview of forecast analysis with arima models during the covid-19 pandemic: Methodology and case study in brazil. Mathematics, 11(14):3069.

Paraschiv, F., Erni, D., and Pietsch, R. (2014). The impact of renewable energies on eex day-ahead electricity prices. Energy Policy, 73:196–210.

Pecinovsky, J. and Boerman, F. (2021). entsoe-py. `https://github.com/EnergieID/entsoe-py` [Online; accessed 2023-01-28].

Radovanović, A., Koningstein, R., Schneider, I., Chen, B., Duarte, A., Roy, B., Xiao, D., Haridasan, M., Hung, P., Care, N., et al. (2022). Carbon-aware computing for datacenters. IEEE Transactions on Power Systems, 38(2):1270–1280.

Riekstin, A. C., Langevin, A., Dandres, T., Gagnon, G., and Cheriet, M. (2018). Time series-based ghg emissions prediction for smart homes. IEEE Transactions on Sustainable Computing, 5(1):134–146.

Schoutsen, P. (2016). Perfect home automation. `https://www.home-assistant.io/blog/2016/01/19/perfect-home-automation/` [Accessed: 2024-02-28].

Seabold, S. and Perktold, J. (2010). statsmodels: Econometric and statistical modeling with python. In 9th Python in Science Conference.

Silva, E. (2024). Handling gaps in time series. `https://towardsdatascience.com/handling-gaps-in-time-series-dc47ae883990` [Accessed 06-04-2024].

Smith, T. G. et al. (2017–). pmdarima: Arima estimators for Python. `http://www.alkaline-ml.com/pmdarima` [Accessed 2024-01-28].

Sørensen, J. (2020). Hacs. `https://hacs.xyz/[Accessed:2023-10-24]`.

Team, H. A. (2020). Electricity maps. `https://www.home-assistant.io/integrations/co2signal` [Accessed: 2024-03-15].

Vaswani, A., Shazeer, N., Parmar, N., Uszkoreit, J., Jones, L., Gomez, A. N., Kaiser, Ł., and Polosukhin, I. (2017). Attention is all you need. Advances in neural information processing systems, 30.

Watttime (2023). Watttime. https://watttime.org/ [Accessed: 2024-03-15].

Wiedemann, J. (2021). apexcharts-card. https://github.com/RomRider/apexcharts-card [Accessed: 2023-10-24].

World Resources Institute (2023). Faq. https://ghgprotocol.org/sites/default/files/standards_supporting/FAQ.pdf [Accessed: 2023-02-15].

Zhang, X. and Wang, D. (2023). A gnn-based day ahead carbon intensity forecasting model for cross-border power grids. In Proceedings of the 14th ACM International Conference on Future Energy Systems, pages 361–373.

A Appendix

A.1 Power sources per TSO zone

TSO zone	Biomass	Fossil Brown & coal/Lignite	Fossil Coal-derived gas	Fossil Gas	Fossil Hard coal	Fossil Oil	Geothermal	Hydro Pumped Storage	Hydro Run-of-river and poundage	Hydro Water Reservoir	Nuclear	Other	Other renewable	Solar	Waste	Wind Offshore	Wind Onshore
DE_50Hertz	+	+	-	+	+	+	+	+	+	-	-	+	+	+	+	+	+
DE_AMPRION	+	+	+	+	+	+	+	+	+	+	+	+	+	+	+	-	+
DE_TENNET	+	+	-	+	+	+	+	+	+	+	+	+	+	+	+	+	+
DE_TRANSNET	+	-	-	+	+	+	-	+	+	+	+	+	+	+	+	-	+

Table 6: Energy sources by TSO zone

A.2 ACF and PACF plots of each TSO zone

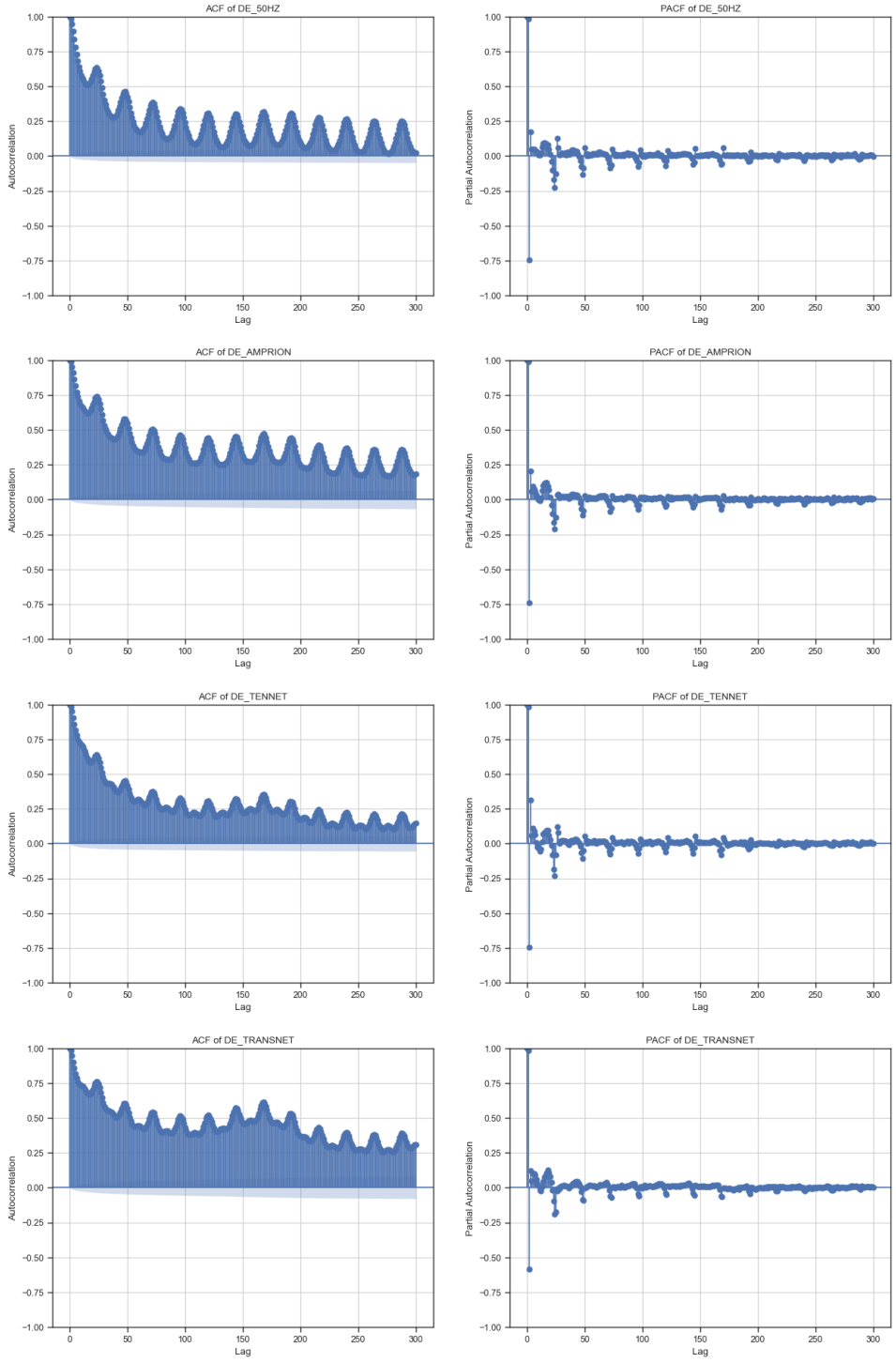

Figure 9: ACF and PACF plots of each TSO zone

A.3 ACF in summer and winter plots of each TSO zone

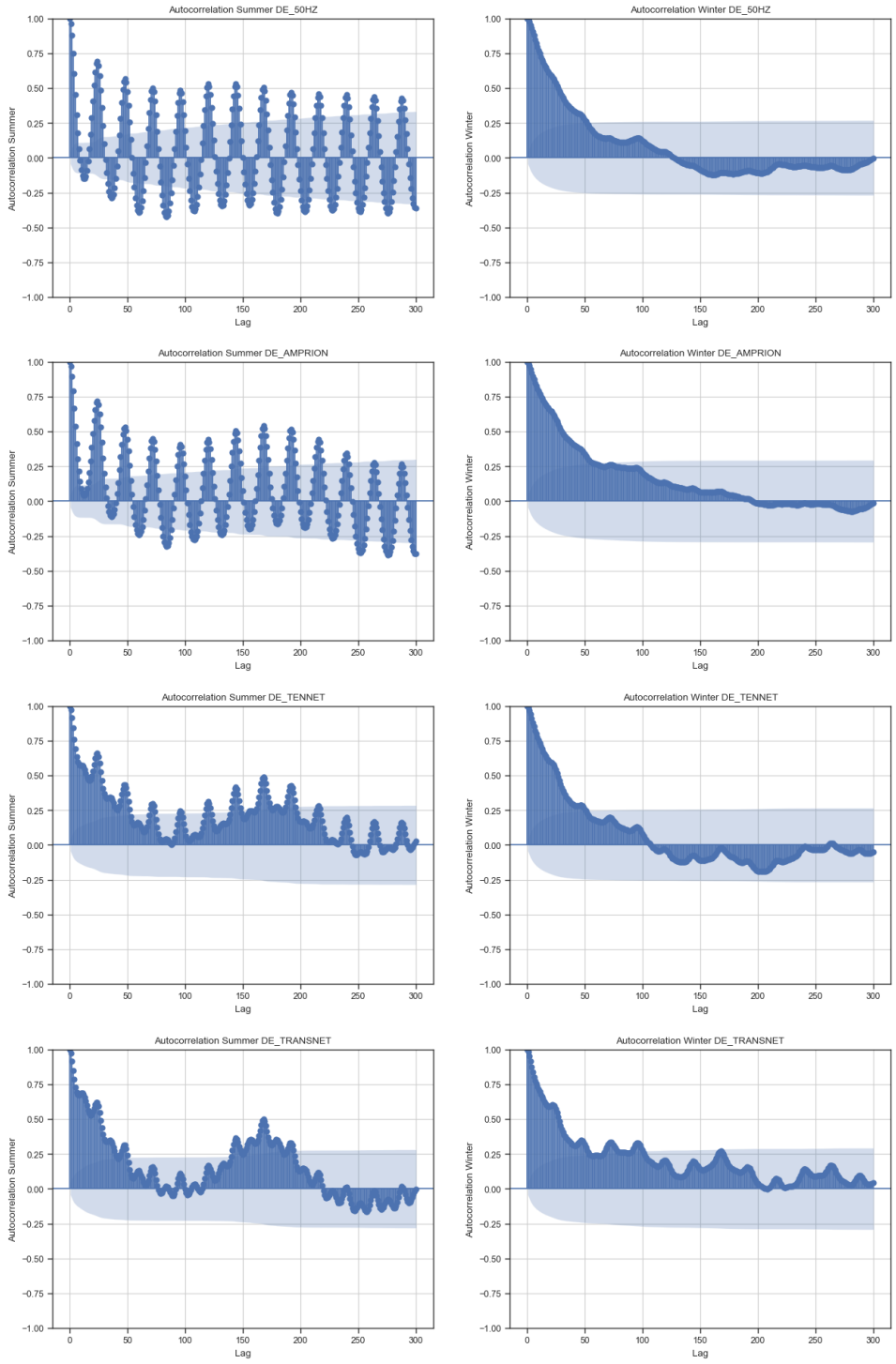

Figure 10: ACF in summer and winter plots of each TSO zone

A.4 Yearly mean carbon intensity and share of renewable energy per TSO zone

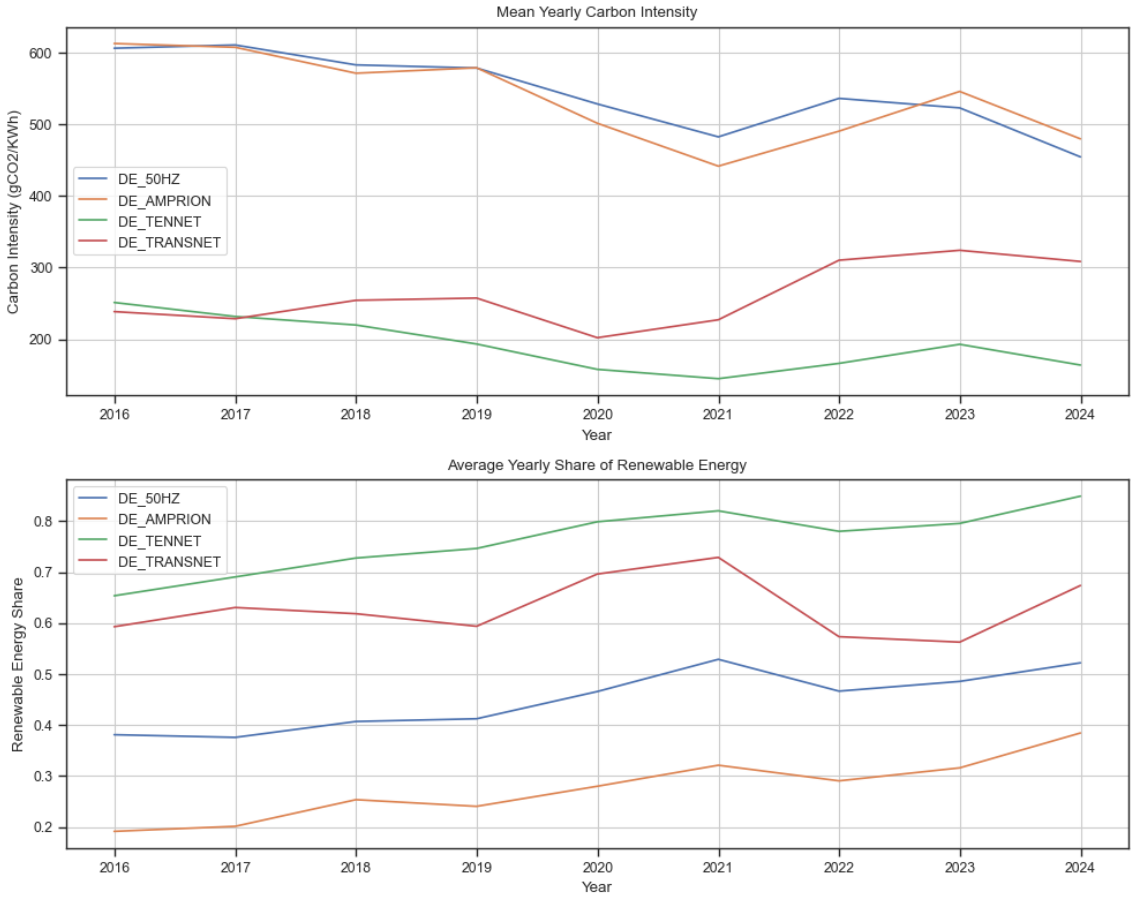

Figure 11: Yearly mean carbon intensity share of renewable energy per TSO zone

A.5 Variable importance plots

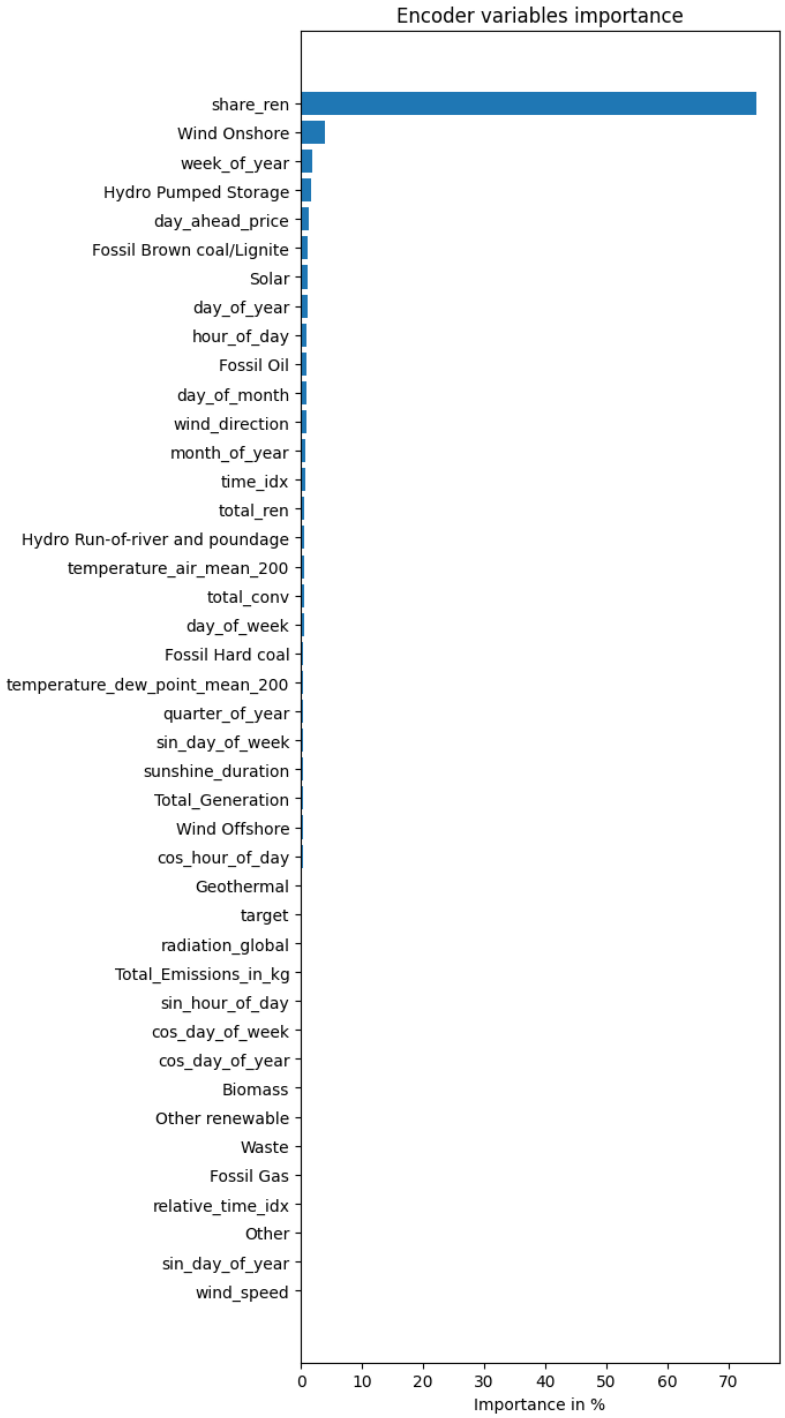

Figure 12: 50Hertz variable importance plot

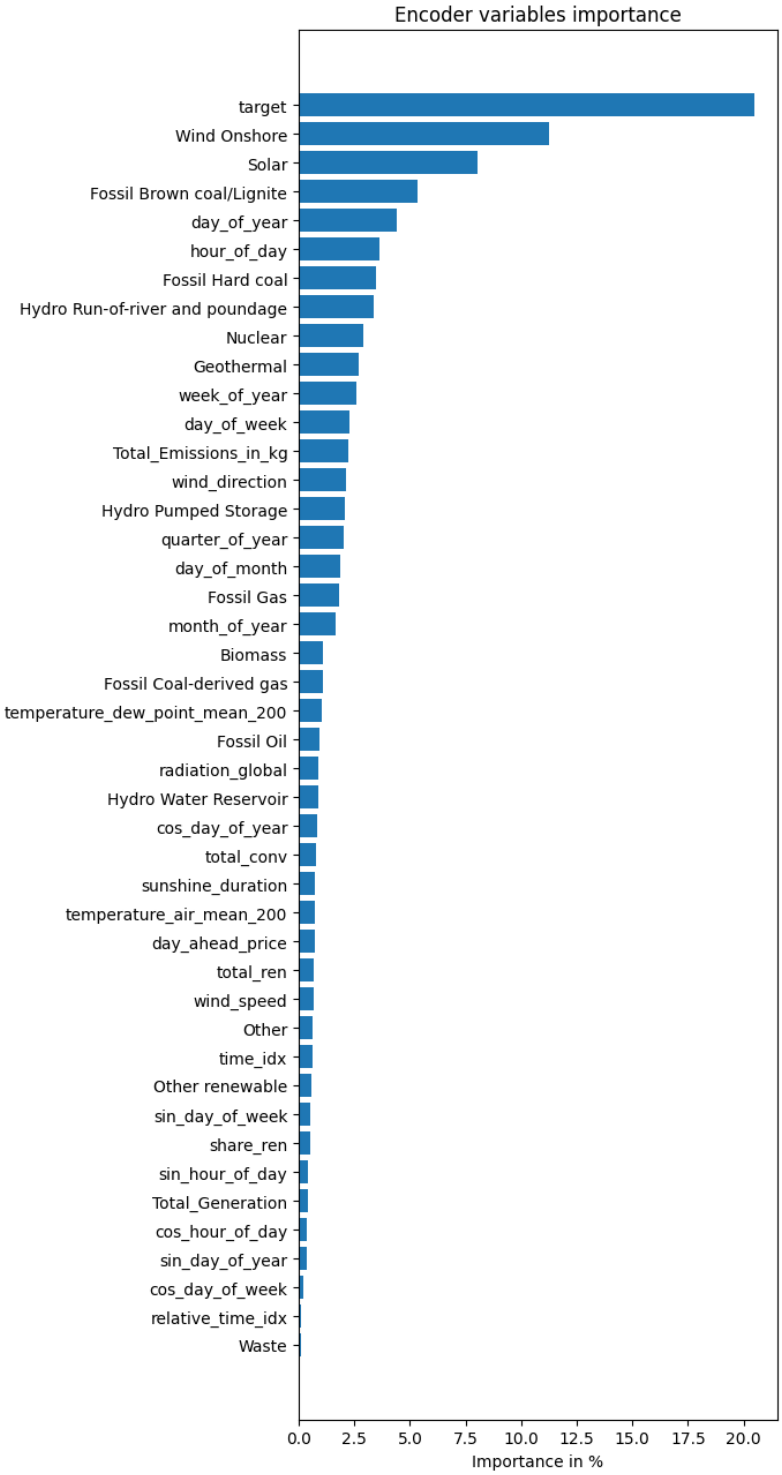

Figure 13: Amprion variable importance plot

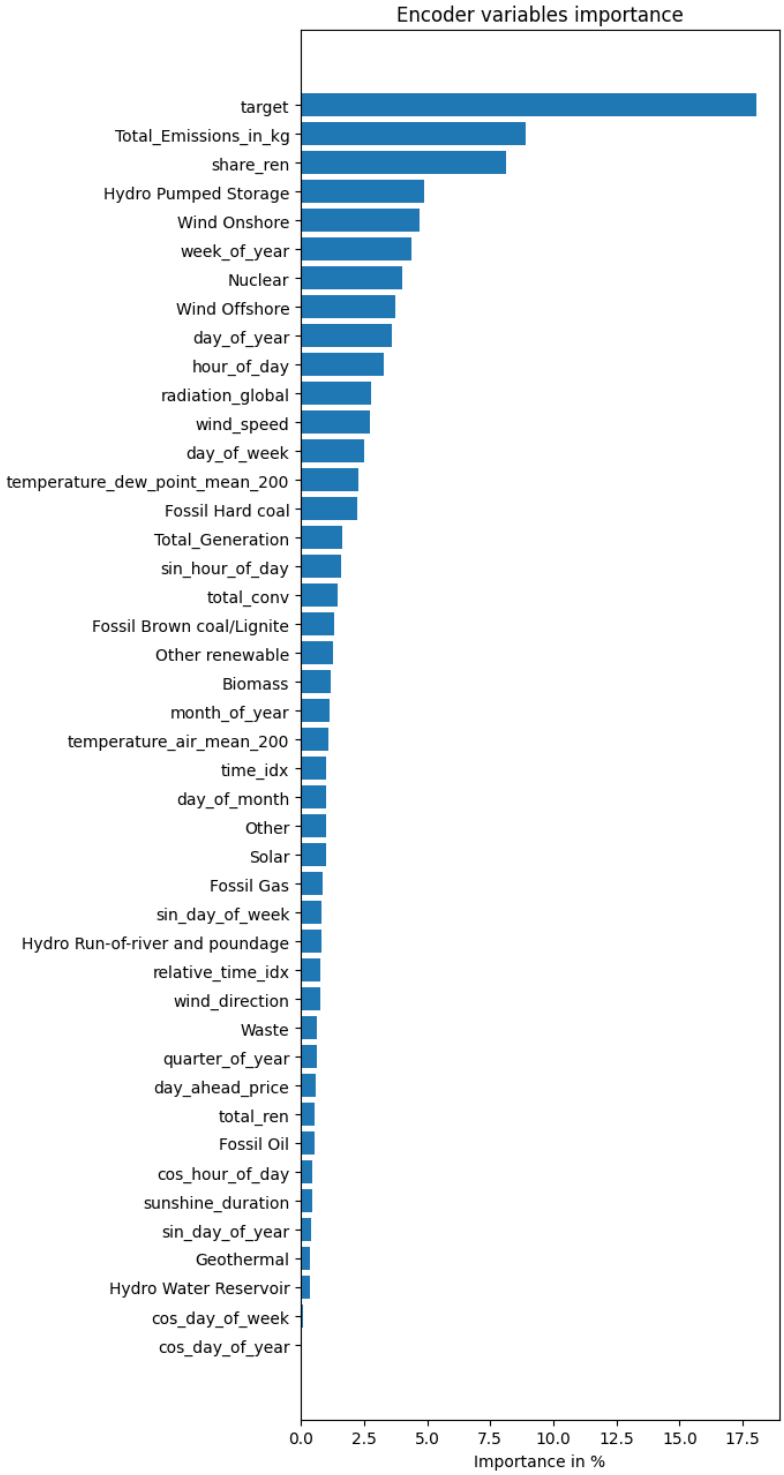

Figure 14: Tennet variable importance plot

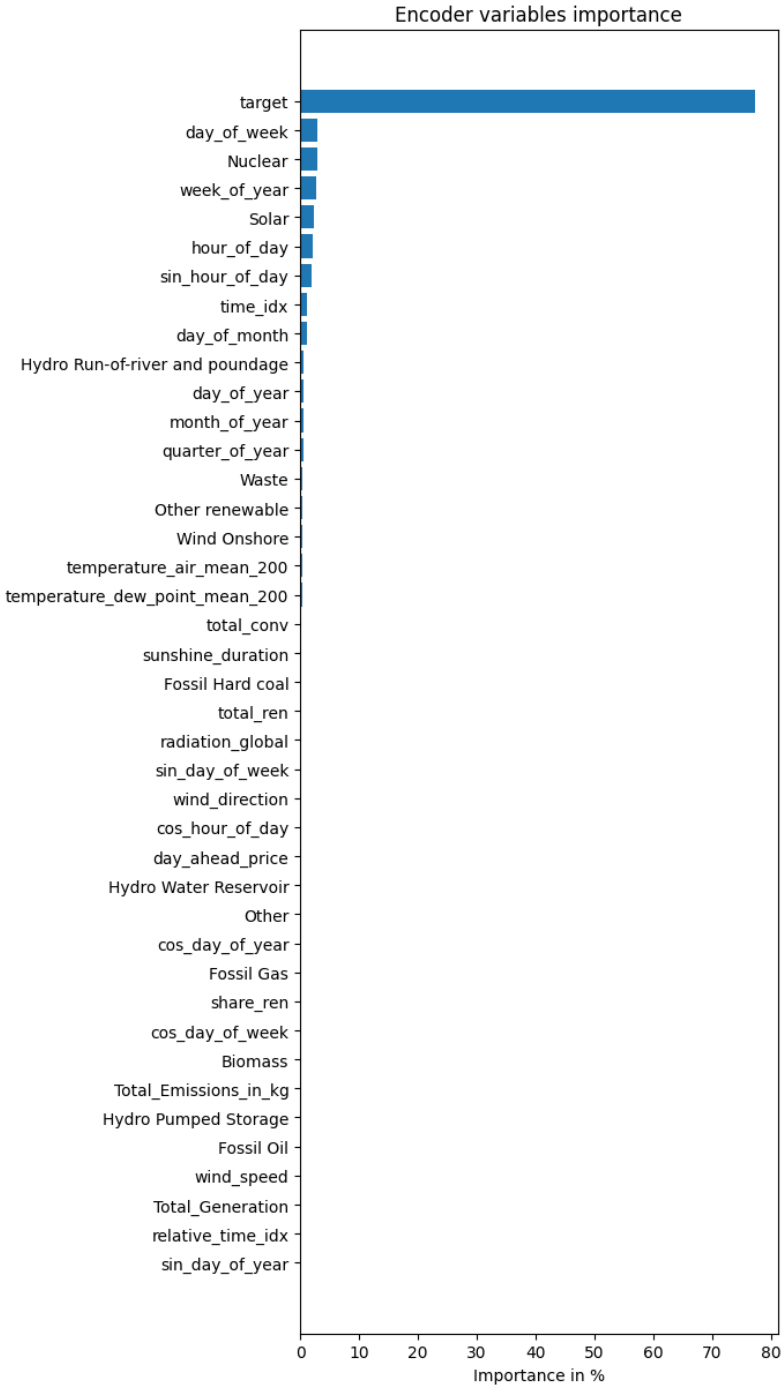

Figure 15: TransnetBW variable importance plot

Declaration of Authorship

I hereby confirm that I have authored this Bachelor's/Master's thesis independently and without use of others than the indicated sources. All passages which are literally or in general matter taken out of publications or other sources are marked as such.

Berlin, May 13, 2024

Carl Tramburg